Accepted Manuscript

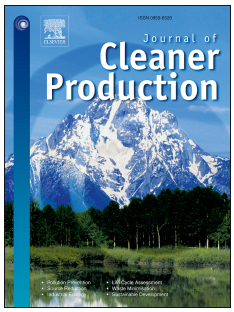

An efficient data delivery and scheduling scheme for smart and sustainable cities

Xu Zhang, Lei Guo, Weigang Hou, Zhaolong Ning, Qihan Zhang, Husheng Li

PII: S0959-6526(19)30044-7

DOI: https://doi.org/10.1016/j.jclepro.2019.01.038

Reference: JCLP 15425

To appear in: *Journal of Cleaner Production*

Received Date: 20 October 2018

Revised Date: 3 January 2019

Accepted Date: 5 January 2019

Please cite this article as: Zhang X, Guo L, Hou W, Ning Z, Zhang Q, Li H, An efficient data delivery and scheduling scheme for smart and sustainable cities, *Journal of Cleaner Production* (2019), doi: https://doi.org/10.1016/j.jclepro.2019.01.038.

This is a PDF file of an unedited manuscript that has been accepted for publication. As a service to our customers we are providing this early version of the manuscript. The manuscript will undergo copyediting, typesetting, and review of the resulting proof before it is published in its final form. Please note that during the production process errors may be discovered which could affect the content, and all legal disclaimers that apply to the journal pertain.

ACCEPTED MANUSCRIPT

An Efficient Data Delivery and Scheduling Scheme for Smart and Sustainable Cities ☆

Xu Zhang[a,b,c], Lei Guo[a,*], Weigang Hou[a,*], Zhaolong Ning[d,*], Qihan Zhang[b], Husheng Li[c,*]

[a]*School of Communication and Information Engineering, Chongqing University of Posts and Telecommunications, Chongqing 400065, China*
[b]*Smart Systems Lab, School of Computer Science and Engineering, Northeastern University, Shenyang 110169, China*
[c]*Department of Electrical Engineering and Computer Science, The University of Tennessee, Knoxville, TN 37996-2250, USA*
[d]*Key Laboratory for Ubiquitous Network and Service Software of Liaoning Province, School of Software, Dalian University of Technology, Dalian, China*

Abstract

With the increasing conflict between population growth and limited environmental resources, building intelligent and efficient data transmission networks is crucial to cleaner production in smart and sustainable cities. More and more people are eager to exchange all kinds of information in urban life through an efficient network. Therefore, designing a smart data distribution and transmission mechanism can not only improve people's quality of life but also pave the way for reducing environmental pollution. Optical networks have been widely used in the core network due to high-capacity characteristics. However, in inter-data-center (Inter-DC) optical networks, the coexisted heterogeneous optical devices and multi-granularity network resources bring new challenges to network management and traffic scheduling. Recently, software-defined network (SDN) and network function virtualization (NFV) have been introduced to enable the unified control for improving network agility and automation. Thus for software-defined multi-granularity Inter-DC optical networks, we propose a list of online service provisioning strategies. Moreover, in terms of the network controller, the novel routing applications are also developed by extended OpenFlow protocol. Finally, we experimentally demonstrate the overall feasibility of proposed solutions in a semi-practical platform. Numerical simulations conducted to quantitatively evaluate the algorithm efficiency also verify the superiorities of improving spectrum efficiency and reducing service blocking probability.

Keywords: Software-defined networks, smart cities, cleaner production, multi-granularity, optical networks.

☆ Fully documented templates are available in the elsarticle package on CTAN.

*Co-corresponding author

Email addresses: zhangxu@stumail.neu.edu.cn (Xu Zhang), guolei@cqupt.edu.cn (Lei Guo), houwg@cqupt.edu.cn (Weigang Hou), zhaolongning@dlut.edu.cn (Zhaolong Ning), zhangqihan@stumail.neu.edu.cn (Qihan Zhang), husheng@eecs.utk.edu (Husheng Li)

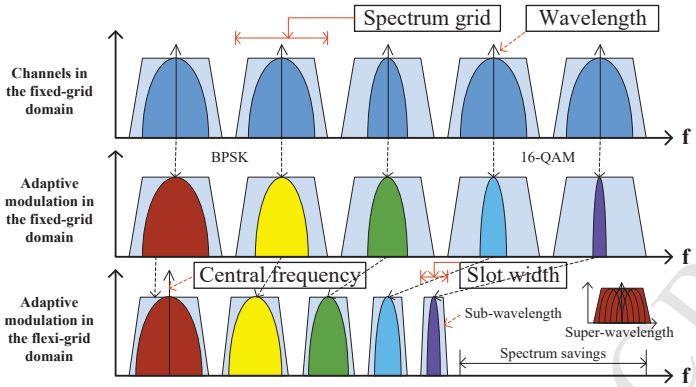

Figure 1: The utilization of heterogeneous multi-granularity spectrum resources.

1. Introduction

Cleaner production is a new and creative idea that continuously takes an overall preventive environmental strategy for production processes and products to reduce their potential hazards to humans and the environment (D. Mark et al. (2018); Y. Fan et al. (2018); H. Shahhosseini et al. (2018)). With the continuous development of human society, the future city will carry more and more people. The increase in population will increase the waste of resources and environmental pollution in cities. Smart cities use information and communication technologies to sense, analyze, and integrate key information in the core systems of urban operations, thereby responding intelligently to the various needs of human activities, aiming to promote sustainable urban development and reduce environmental pollution. Meanwhile, the rapid update of new technologies has injected a large amount of data into the network, especially in 5G (C. Wang et al. (2014)), Internet of Things (IoT) (P. Ramezani et al. (2017)) and smart phone applications (W. Hou et al. (2018a)). The birth of big data (L. Cui et al. (2016); W. Hou et al. (2017b)) further promotes the development of cloud computing (Y. Yin et al. (2017); L. Guo et al. (2018)) that provides users with a lot of computing resources at low investment. Especially, the combination of cloud computing and network function virtualization (NFV) have achieved temporal and spacial flexibilities of physical devices. However, as the size of server clusters continues to expand, cloud computing platforms consist of geographically dispersed data centers (DCs) (P. Lu et al. (2017); W. Hou et al. (2018b)) communicating with each other through fast and high-capacity optical networks. Inter-DC optical networks are equipped with heterogeneous devices and multi-granularity resources, such as wavelength division multiplexing (WDM) and orthogonal frequency division multiplexing (OFDM) (L. Gong et al. (2014)). This paper focuses on designing efficient optical networks to serve data communication among data centers, aiming to explore solutions that contribute to smart and sustainable urban development.

1.1. Motivation

Figure 1 shows the utilization of heterogeneous multi-granularity spectrum resources. The optical-to-electrical-to-optical (O/E/O) conversion is needed to support highly dynamic traffic in a WDM network, hence we call it as the opaque fixed-grid optical network. The elastic optical network (EON) based on OFDM technology is the transparent flexi-grid optical network with

ACCEPTED MANUSCRIPT

the use of all-optical technology. On the other hand, there are different levels of modulation formats, such as binary phase shift keying (BPSK), quadrature phase shift keying (QPSK), 8-ary quadrature amplitude modulation (8-QAM), and 16-QAM. Note that, a high-level modulation format has a short transmission distance, and vice visa (K. Walkowiak et al. (2017)).

In a fixed-grid WDM network, the spectrum bandwidth of each channel is fixed. However, one channel can accommodate different capacities using different modulation formats. Therefore, the capacity requirement of less than one full wavelength will result in the bandwidth waste. Unlike WDM networks, the introduction of adaptive modulation format in EONs also improves the spectral efficiency. EONs also can allocate a certain number of subcarriers according to the user's requirement, which reduces the granularity of network resources to the sub-wavelength. More importantly, EONs increase the efficiency of the spectrum by creating the super wavelength if the large-capacity service requests cannot be provided by a single channel.

The coexist of aforementioned heterogeneous technologies and multi-granularity network resources bring new challenges to the unified management and flexible traffic scheduling of inter-DC optical networks. For multi-granularity inter-DC optical networks in future, these challenges include how to differentiate and control different types of traffic and to uniformly allocate multi-granularity network resources for different network scenarios. The most important difficulty in solving these challenges is both the construction of a centralized network architecture and the design of hybrid routing algorithms. Therefore, the root cause of the inability of the existing distributed solution to perform fine-grained level traffic control is the lack of a global network view.

The software-defined network (SDN) (D. Kreutz et al. (2015); A. Thyagaturu et al. (2016))—that enables the separation of control and data forwarding planes—promotes the flexible centralized and fine-grained control of network traffic (X. Zhang et al. (2017a)), and meanwhile, it provides unprecedented programmability, automation (X. Zhang et al. (2017b, 2016)), and control capabilities for the network (Z. Zhu et al. (2018); L. Li et al. (2017); Z. Zhu et al. (2015)). Furthermore, benefit from the centralized control mechanism and data plane whiteboxing trend, OpenFlow can program the entire network to achieve the virtualization of IP routers, Ethernet switches, and even optical switching nodes such as bandwidth-variable optical cross-connects (BV-OXCs), bandwidth-variable wavelength selective switches (BV-WSSs) and edge routers (ERs). Therefore, the OpenFlow-based network control and management plane is very suitable for heterogeneous and multi-granularity Inter-DC optical networks (P. Lu et al. (2017)).

1.2. Contribution

In this paper, we focus on designing software-defined multi-granularity inter-DC optical networks so that we can greatly enhance the network controllability and flexibility, and effectively reduce the costs of investment and operational management. Especially, we solve the problem of spectrum planning and traffic scheduling in software-defined multi-granularity inter-DC optical networks (SPTS-SDMGON). Unlike the spectrum planning and traffic scheduling schemes in other papers, our approach is more complete. It can distinguish different types of traffic from different scenarios and offload it to the matching resource allocation scheme. This greatly enhances the effectiveness of heterogeneous network resource allocation. At the same time, thanks to the advantages of the SDN architecture, we are able to provide an application-level docking in the management plane by extending the OpenFlow protocol for multi-granularity inter-DC optical network scenarios. More specifically, we first elaborate on the overall network architecture, and extend the OpenFlow protocol to implement the seamless operation between control and data

ACCEPTED MANUSCRIPT

planes. Next, the mathematical problem of allocating heterogeneous network resources is formulated. For transparent flexi-grid optical networks, we maximize the spectral efficiency and the connectivity based on the lightpath with adaptive modulation level selection (MSECML). For opaque fixed-grid optical networks, we select the lightpath with the maximized capacity-over-hops first (MCHF) from virtual network slices. Heuristic algorithms are then proposed to solve the problem of resource allocation and lightpath computing. Note that, well-designed weights and maximum flow algorithms are utilized to build virtual network slices between source and destination nodes, which helps us to find the optimal traffic scheduling scheme in real time according to dynamic link load. Moreover, we develop multi-granularity routing applications by extending the RYU controller. Finally, we implement our solution in a semi-practical system testbed. The overall feasibility and efficiency of the proposed solution are experimentally verified and evaluated based on the NSFNET topology. The major contributions of this paper are in the following:

1. The overall architecture of software-defined multi-granularity inter-DC optical networks is designed, and we formulate the problem of SPTS-SDMGON.
2. MSECML and MCHF algorithms are designed for the transparent flexi-grid optical network and the opaque fixed-grid optical network, respectively, and their time complexity is also analyzed.
3. The software-defined multi-granularity routing applications are proposed to demonstrate the feasibility of the overall solution, and the extended OpenFlow protocol is utilized for controlling optical devices.
4. We evaluate the performance of proposed algorithms in a semi-practical platform, and the result of the experiment well proves the effectiveness of our schemes.

The rest of the paper is organized as follows. Section 2 provides a brief survey on the related work. Then, we describe the overall network architecture, network model, and problem formulation in Section 3. Heuristic algorithms are discussed in Section 4. Next, Section 5 presents the system implementation, experimental demonstration and performance evaluation. Finally, we summarize the paper in Section 6.

2. Related Work

For fixed-grid WDM networks, the routing and wavelength assignment (RWA) algorithms have been widely researched in literatures. In L. Liu et al. (2011), Liu et al. experimentally demonstrated an OpenFlow-based control plane to provide lightpaths in the transparent optical network. In G. Shen et al. (2009), Shen et al. designed energy-efficient network architectures, and developed operational strategies to reduce the energy consumption of WDM optical networks. To solve the survivable problem, dynamic routing and virtual network embedding (VNE) algorithms were also proposed to keep a survivable network topology in B. Guo et al. (2011). For the green optical network (L. Guo et al. (2013)), Guo et al. formulated the problem of green many-to-many routing in WDM optical networks. They designed a rational combined method of lightpaths to improve the energy efficiency of the WDM network. In A. Coiro et al. (2014), Coiro et al. considered the problem of optical signal transmission impairments, and developed the energy efficiency RWA algorithms in transparent WDM networks. Q. Zhang et al. (2013) jointly considered the problems of VNE and RWA in WDM optical networks. In addition, W. Hou et al.

(2017a) focused on a risk-aware VNE architecture, and designed a risk-aware heuristic algorithm to perform security physical isolation from risky virtual machines. However, these studies allocate fixed-grid resources, leading to the spectral waste.

For flexi-grid OFDM networks (e.g., EONs), traffic grooming and spectrum allocation were studied for the dynamic service provisioning in (F. Musumeci et al. (2013); Z. Zhu et al. (2013); W. Lu et al. (2013); A. N. Patel et al. (2013); X. Wan et al. (2012); Y. Wang et al. (2013)). For instance, Z. Zhu et al. (2013) proposed several online routing, modulation level and spectrum assignment algorithms based on a hybrid single-/multi-path routing scheme. In A. N. Patel et al. (2013), Patel et al. designed a QoS-aware protocol for the optical burst switching in an OpenFlow-based software-defined optical network. For the survivable problem in EONs, L. Ruan et al. (2013) provided flexible protection levels by utilizing survivable multiple lightpaths in OFDM-based EONs. In X. Chen et al. (2015), Chen et al. took the advantages of failure-independent pre-configured cycles (FIPP p-cycles) for path protection and investigated the methods of realizing spectrum-efficient resilience design based on the above idea. In addition, J. Vizcano et al. (2012) analyzed the energy efficiency of the flexi-grid OFDM-based solution in the dynamic network considering time-varying connections. J. Wang et al. (2013) designed an overlay general multi-protocol label switching model to collect global network information based on SDN architecture, which could improve the energy efficiency of the wider areas' network. However, these studies do not consider the scenario of heterogeneous multi-granularity optical networks among DCs.

L. Liu et al. (2013b) presented the dynamic end-to-end lightpath provisioning and IP traffic offloading scheme in spectrum sliced EONs. Then, in L. Liu et al. (2013a), they reported an OpenFlow-based control plane in software-defined and multi-layer optical networks, and they verified the overall feasibility, efficiency, and the end-to-end latency for lightpath creation and restoration. M. Channegowda et al. (2013) reported the novel OpenFlow-based control plane, which could implement the seamless operation between optical and packet transport domains. Moreover, Zhang et al. proposed and implemented a novel EON-based enhanced SDN architecture for the DC application in J. Zhang et al. (2013) and H. Yang et al. (2015), respectively. These studies are helpful to our work because they have verified the feasibility of deploying the SDN in inter-DC optical networks from the experimental point of view. As shown in Fig. 1, different spectrum granularities, modulation formats and data multiplexing techniques exist together in the future inter-DC optical network, which makes the multi-granularity routing application of the SDN controller very necessary. However, the existing works mentioned in this paragraph do not perform the traffic scheduling from the multi-granularity routing applications perspective.

3. Network Architecture and Problem Description

In this section, we first describe the overall network architecture and design the corresponding network model. The SPTS-SDMGON problem is then formulated mathematically.

3.1. Network Architecture

Figure 2 shows the architecture of software-defined multi-granularity inter-DC optical networks, which includes data plane, control plane and management plane.

In the data plane, the switching granularities are wavelength, sub-wavelength and super-wavelength for fixed-grid WDM and flexi-grid OFDM networks. The fixed-grid BV-OXCs and

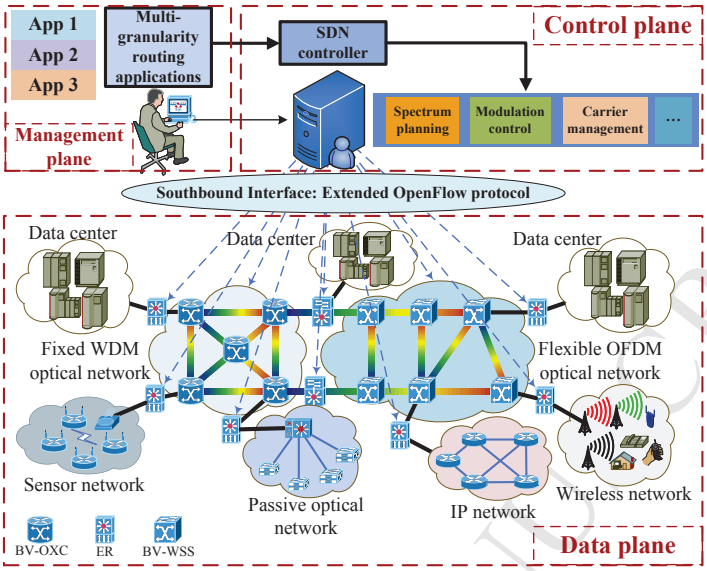

Figure 2: Software-defined multi-granularity inter-DC optical networks.

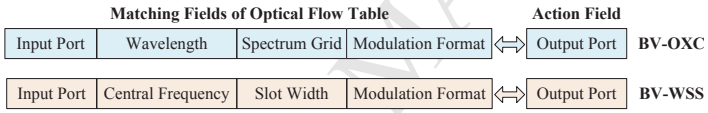

Figure 3: Optical flow tables.

flexi-grid BV-WSSs can respectively switch wavelengths and contiguous spectrum slots to the correct destination port. Leveraging bandwidth-variable transponders (BV-Ts) and spectrum (de)multiplexer (MUX/DEMUX), ERs have the ability to (un)load client traffic. For instance, ERs sent traffic from IP networks, sensor networks, passive optical networks (PONs) and wireless networks to the DC. The data transfer among DCs is also accomplished by ERs.

The extended OpenFlow 1.3 protocol is exploited to support the communication between control and data planes. More specifically, we add optical attributes to the existing flow table, and the extended optical flow table consists of match fields, action fields, and associated counter fields (L. Liu et al. (2011, 2013b)). Unlike the standard OpenFlow protocol, our extended optical flow tables are for heterogeneous multi-granularity optical network scenarios. Figure 3 shows the matching and associated action fields for the flow table characterizing the rules of operating BV-OXCs and BV-WSSs, respectively. Because some current optical devices do not well support the extended OpenFlow protocol above, the controller communicates with the OpenFlow agent (OF-AG) attached to BV-WSS and BV-OXC. The OF-AG configures the optical equipment according to the controller's instructions, and it collects the status information of optical devices to inform the controller. When a service requirement arrives at the ER, the related OF-AG sends the Packet-In message to the controller. The controller then calculates a proper route based on the multi-granularity routing application deployed in the management plane, and it distributes Flow-Mod messages to related OF-AGs for the lightpath establishment. Note that, since the

multi-granularity routing applications we developed are in the management plane layer, then the management plane is sitting at the application layer.

3.2. Network Model

In software-defined multi-granularity inter-DC optical networks, there are transparent flexi-grid and opaque fixed-grid optical networks modeled separately in the following.

The transparent flexi-grid optical network (EON) can be modeled by a directed graph $G(V, E)$, where V is the set of BV-WSSs, and E is the set of bidirectional fiber links. Each fiber link $e(u, v) \in E, \forall u, v \in V$ accommodates N frequency slots, and D is the set of all possible link lengths $l_e \in D, \forall e \in E$. The subcarrier bandwidth is $B_{FS} = 12.5$ GHz, and there is the bandwidth of B GHz on each fiber link. Therefore, the initial number of frequency slots on every fiber link is $N = \lfloor B/B_{FS} \rfloor$. The subcarrier capacity is $C_{BPSK} = 2 \times B_{FS} = 25$ Gbps based on the Nyquist first criterion when using BPSK modulation format (i.e., modulation level $m = 1$). For different modulation levels, a single subcarrier transmission bit rate equals to $(m \cdot C_{BPSK})$ Gbps. We also define a bit-mask $bm_{e,j}$ that contains N bits to describe the utilization status of frequency slots on the fiber link e. $bm_{e,j} = 1$ represents the j^{th} frequency slot on the fiber link e is used, otherwise it is 0.

The opaque fixed-grid (WDM) optical network is denoted by another directed graph $G'(V', E')$ where V' represents a set of BV-OXCs, and E' is the set of bidirectional fiber links. Each fiber link can accommodate the bandwidth of B' in GHz at most, while the spectrum is divided into W wavelengths. For instance, the fixed granularity of WDM channels is $B'_\lambda = 50$ GHz, we can derive $W = \left\lfloor B'/B'_\lambda \right\rfloor$. To support highly dynamic traffic, O/E/O conversion is required to forward the optical data to electrical layer. It is different from the transparent domain. Moreover, the wavelength conversion can be performed at the intermediate node between two different links in the lightpath.

A service requirement is represented by a 4-tuple model $r(s, d, x, b_x), \forall r \in R$, where s is the source node, and d is the destination node. Variable x denotes the type index of the multi-granularity service request: $x = 0$ for the flexible granularity in the transparent domain while $x = 1$ for the fixed granularity in the opaque domain. Variable b_0 represents the capacity requirement of the flexi-grid service request in the transparent domain, while b_1 denotes the capacity requirement of the fixed-grid service request in the opaque domain. According to Eq. (1), we can derive the number of contiguous spectrum slots n allocated to the service request r with the assigned modulation level m. Here, g represents the guard bandwidth usually set to one spectrum slot. All service requests have the same requirement of link bandwidth in opaque fixed-grid optical networks (W. Hou et al. (2017a)), i.e., $b_1 = OC\_1$.

$$n = \left\lceil \frac{b_0}{m \cdot C_{BPSK}} \right\rceil + g. \tag{1}$$

In addition, the lightpath can select its modulation level adaptively according to the transmission distance. We assign the modulation level $m = \{1, 2, 3, 4\}$ for BPSK, QPSK, 8-QAM, and 16-QAM, respectively. When the transmission distance of the lightpath p is known, the modulation level m is shown in Eq. (2) where $Hml(\cdot)$ returns the highest modulation level according to the relationship between modulation level and maximum transmission reach (X. Zhang et al. (2017a)).

$$m = Hml\left(\sum_e l_e\right), \forall e \in p, \forall l_e \in D. \tag{2}$$

ACCEPTED MANUSCRIPT

3.3. Problem Formulation

Based on the network models above, we investigate the corresponding dynamic service provisioning problem. Some important notations and variables are listed Tables 1 and 2, respectively.

First, we define the capacity of the fiber link as $c(u, v), \forall u, v \in V$, and the flow value of a link is the bandwidth capacity consumed by the traffic passing through this link, i.e., $f(u, v)$. Then, the residual capacity of the link $c_f(u, v) = c(u, v) - f(u, v), \forall u, v \in V$. Given the network graph G and flow f, the residual network graph G_f consists of edges that still have space to adjust traffic requests. Therefore, the residual network G induced by the flow f is $G_f = (V, E_f)$, where $E_f = \{(u, v) \in V \times V : c_f(u, v) > 0\}$.

$$\text{Min } R - \sum_{r} \sum_{p} \sum_{e} \sum_{i} \alpha_p^r \varphi_{e,i}^r. \tag{3}$$

Next, we design a mix of algorithms application to enhance the intelligence of the control plane. The goal of our algorithms is to minimize the traffic blocking rate with Eq. (3). Next, considering the respective characteristics of traffic in EON and WDM networks, we further give the different optimization strategies for two types of networks. For transparent EONs, since the number of spectrum slots for service requests is varied, we maximize the connectivity of all available spectrum slots to satisfy subsequent service requests as many as possible, which is shown in Eq. (4); For opaque WDM networks, since the traffic demand is a single wavelength, we minimize the index number of the used wavelength to minimize the traffic blocking rate, which is shown in Eq. (23). In summary, we solve the EONs/fixed-grid optical network cases independently by using aforementioned two strategies in Algorithm 1 but with the same optimization objective, i.e., to minimize the traffic blocking rate.

$$\text{Max} \sum_{r \in R} \sum_{e \in E} \left(N_e^{points} \cdot N_e^{slots}\right) / \left(N_e^{blocks} \cdot N\right), \tag{4}$$

$$N_e^{slots} = \sum_{j=1}^{N} \left(1 - bm_{e,j}\right), \forall e \in E, \tag{5}$$

$$N_e^{points} = \sum_{j=1}^{N-1} \left(1 - bm_{e,j}\right) \cdot \left(1 - bm_{e,j+1}\right), \forall e \in E, \tag{6}$$

$$N_e^{blocks} = N_e^{slots} - N_e^{points}, \forall e \in E. \tag{7}$$

We obtain the values of N_e^{slots}, N_e^{points} and N_e^{blocks} according to Eqs. (5), (6) and (7), respectively. Here, N_e^{slots} denotes the number of available spectrum slots on the fiber link e. N_e^{points} indicates the number of connection points between free spectrum slots on the fiber link e. N_e^{blocks} represents the number of available spectrum blocks on the fiber link e. A larger objective function value means the higher contiguity of frequency slots, i.e., the more available spectrum resources for service requests to arrive. Therefore, the network is able to provide more services by using optimization guidelines.

The above-mentioned objective should satisfy some constraints as follows:

$$\sum_{p \in P} \alpha_p^r \leq 1, \forall r \in R, \tag{8}$$

$$\sum_{i} \varphi_{e,i}^{r} = \beta_{e}^{r} \leq 1, \forall r \in R, \forall e \in E. \tag{9}$$

Equations (8) and (9) ensure that each service request can select only one lightpath and only one spectrum block on the fiber link.

$$z^{r} - w^{r} + 1 = \sum_{p} \alpha_{p}^{r} \cdot \left\lceil \frac{b_0}{m \cdot C_{BPSK}} \right\rceil, \ \forall r \in R. \tag{10}$$

Equation (10) ensures that the number of frequency slots assigned to each service request must satisfy the corresponding capacity requirement.

$$w^{r} \geq w_{e,i} \cdot \left(\beta_{e}^{r} + \varphi_{e,i}^{r} - 1\right), \forall r \in R, \forall e \in E, \forall i, \tag{11}$$

$$z^{r} - z_{e,i} \leq N \cdot \left(2 - \beta_{e}^{r} - \varphi_{e,i}^{r}\right), \forall r \in R, \forall e \in E, \forall i. \tag{12}$$

Equations (11) and (12) guarantee that the spectrum slots required by the service request should be located in the i^{th} spectrum block on the fiber link.

$$\sigma^{r_1,r_2} + \sigma^{r_2,r_1} = 1, \forall r_1, r_2 \in R. \tag{13}$$

Equation (13) determines the order of service requests r_1 and r_2 on the common fiber link.

$$z^{r_2} - w^{r_1} + 1 \leq N \cdot (1 + \sigma^{r_1,r_2} - \pi^{r_1,r_2}), \forall r_1, r_2 \in R, \tag{14}$$

$$z^{r_1} - w^{r_2} + 1 \leq N \cdot (2 - \sigma^{r_1,r_2} - \pi^{r_1,r_2}), \forall r_1, r_2 \in R. \tag{15}$$

Equations (14) and (15) mean that the spectrum assigned to service requests r_1 and r_2 satisfies the spectrum non-overlapping constraint (Z. Zhu et al. (2013)).

$$\pi^{r_1,r_2} \geq \alpha_{p_1}^{r_1} + \alpha_{p_2}^{r_2} - 1, \forall r_1, r_2 \in R, \forall p_1, p_2 \in P_e. \tag{16}$$

Equation (16) represents that the lightpath p_1 serving the request r_1 and p_2 serving r_2 have common fiber links.

$$0 \leq f(u,v) \leq c(u,v), \forall u, v \in V. \tag{17}$$

Equation (17) ensures that the number of flows through the fiber link is less than or equal to the link capacity.

$$\sum_{v \in V} f(u,v) = \sum_{v \in V} f(v,u), \forall u \in V - \{s,d\}. \tag{18}$$

Equation (18) ensures that the numbers of input and output flows are equal on each intermediate node.

$$\sum_{u \in V} f(u,s) = 0. \tag{19}$$

ACCEPTED MANUSCRIPT

Equation (19) ensures that the number of input flows to the source node equals to 0.

$$\sum_{v \in V} f(d, v) = 0. \tag{20}$$

Equation (20) ensures that the number of output flows from the destination node equals to 0.

$$\sum_{v \in V} f(s, v) = \sum_{r \in R} b_x, \forall s \in r, \tag{21}$$

$$\sum_{u \in V} f(u, d) = \sum_{r \in R} b_x, \forall d \in r. \tag{22}$$

Equations (21) and (22) guarantee that the number of output flows from the source node equals to the number of input flows to the destination node.

For opaque fixed-grid optical networks, due to the introduction of O/E/O conversions, we ignore the constraint of the wavelength contiguousness. Therefore, the corresponding objective of the service provisioning is to minimize the blocking probability of services. The first term in the objective function (Eq. (23)) minimizes the total index of the used wavelength. The second term reduces the total number of O/E/O conversions.

$$\text{Min} \sum_{r \in R} \xi^r_{e,\lambda} \cdot \lambda + \sum_{r \in R} \psi^r_e. \tag{23}$$

The objective above should satisfy constraints of bandwidth capacity and wavelength continuity as follows:

$$\sum_{r \in R} \sum_{\lambda=1}^{W} \xi^r_{e,\lambda} \leq W, \forall e \in E'. \tag{24}$$

Equation (24) is the bandwidth capacity constraint. It indicates that the maximal number of service requirements on the fiber link is constrained by the total number of wavelengths.

$$\sum_{\lambda=1}^{W} \xi^r_{e,\lambda} \leq 1, \forall r \in R, \forall e \in E'. \tag{25}$$

Equation (25) is the wavelength continuity constraint, which means that only one wavelength λ in the fiber link e can be allocated for the service requirement r.

The lightpath routing and resource allocation in the flexi-grid optical network is NP-hard, which has been proved in our previous work (X. Zhang et al. (2017a)). The problem here is more complex since it also includes the fixed-grid domain. Therefore, our problem is NP-hard.

4. Heuristic algorithms and routing applications

Since our SPTS-SDMGON problem is NP-hard by nature, we propose heuristic algorithms to solve it. Furthermore, we develop the software-defined multi-granularity routing application by extending the SDN controller.

ACCEPTED MANUSCRIPT

Algorithm 1: Main Body

Input: Substrate networks G and G', service request r.
Output: Lightpath, central frequency/wavelength, slot width/spectrum grid, modulation level.

```
1  for each request r(s, d, x, b_x) in R do
2      query the access table to determine s and d
3      if s = null or d = null then
4          block r
5      else
6          if x = 0 then
7              apply Algorithm 2
8          end
9          if x = 1 then
10             apply Algorithm 3
11         end
12     end
13 end
```

4.1. Heuristic Algorithms

In this subsection, we propose several efficient algorithms to solve the problem of dynamic service provisioning in software-defined and multi-granularity inter-DC optical networks.

Algorithm 1 depicts the overall procedure of our multi-granularity routing algorithm (MGRA). The for-loop that covers lines 1-13 provides the network service for each request. Line 2 determines the location of source and destination nodes by querying the access table (X. Zhang et al. (2017a)). If not found, the service request is blocked. Lines 5-12 identify the type of the service request. Apply **Algorithm 2** if it is a flexi-grid request, otherwise apply **Algorithm 3** for the fixed-grid request. In the following, we design **Algorithms 2** and **3** to provide high-quality and efficient services for the multi-granularity optical network.

Algorithm 2 is designed to improve the spectral efficiency and the connectivity of all available spectrum slots. Lines 2-6 calculate K candidate lightpaths for each flexi-grid request based on the underlying residual network graph, and store paths in the set P. In line 2, the edge weight of the network graph is deliberately set to search available resources as many as possible. Lines 7-25 are the process of spectrum allocation for candidate paths. To satisfy the spectrum contiguousness constraint in the transparent flexi-grid optical network, line 9 makes a bitwise AND operation for all the fiber links in a lightpath with Eq. (26). Based on the path length, the modulation format is determined in line 10. After knowing the modulation format, we calculate the number of frequency slots required by a service request according to Eq. (1). Line 12 checks whether the block of n contiguous frequency slots is available or not in the lightpath. If yes, we store the *block* in the set *blocks*. By the end of line 12, all available frequency blocks in the lightpath are stored in the set *blocks*. We then pre-allocate n spectrum slots to each spectrum block, and compute the objective function value in lines 16-19. Of course, we will block the service request if there are no available spectrum blocks in all candidate lightpaths. Finally, we choose the spectrum block with the largest objective function value and determine the central frequency, and meanwhile, optical flow entries are generated to insert related OF-AGs for the

ACCEPTED MANUSCRIPT

Algorithm 2: MSECML

Input: Substrate network G, service request r.
Output: Lightpath p, central frequency, slot width n, modulation level m.

```
for each request r(s, d, b_0) do
    set edge weight = l_e / N_e^slots, ∀e ∈ E
    for 1 to k do
        p = Dijkstra(s, d, weight) in the substrate network graph G(V, E)
        P = {p}
    end
    if P ≠ ∅ then
        for each path p in P do
            compute path status with Eq. (26)
            select modulation level m with Eq. (2)
            calculate the number of spectrum slots n with Eq. (1)
            search the available spectrum blocks for n spectrum slots
            if blocks is empty then
                block r
            else
                for each block in blocks do
                    pre-allocate n to the spectrum block
                    select Max(block) based on Eq. (4)
                end
            end
        end
        select lightpath and spectrum block
        determine the central frequency
        insert flow entries to related OF-AGs
    end
    if P = ∅ then
        block r
    end
end
```

lightpath establishment.

$$bm_{p,j} = \bigcap_{e} bm_{e,j}, \forall e \in p. \tag{26}$$

Algorithm 3 shows the detailed procedure of the service provision for the opaque fixed-grid request. Since optical switching nodes have O/E/O conversion capabilities in an opaque WDM optical network, we can use wavelengths on different fiber links along the lightpath. However, O/E/O conversions can increase the end-to-end latency. Hence, we minimize the traffic congestion with slight O/E/O conversions. Different from transparent optical networks, we construct the layer of the auxiliary graph with source and destination nodes for each service request, and transform this process into the minimum-cost maximum-flow (MCMF) problem (P. Lu et al. (2017)).

ACCEPTED MANUSCRIPT

Algorithm 3: MCHF

Input: Substrate network G', service request r.
Output: Lightpath p', wavelength λ, spectrum grid, modulation level m.

```
1  for each request r(s, d, b_1) do
2      P' = ∅
3      P=execute Algorithm 4 for request r
4      for each path p in P do
5          if b_1 ≤ c_f(p) then
6              P' = {p}
7          end
8      end
9      if P' = ∅ then
10         block r
11     else
12         p' = Max(c_f(p'), ∀p' ∈ P'), or
13         p' = Max(c_f(p')/hop(p'), ∀p' ∈ P'), or
14         p' = Min(Σ_e l_e, ∀e ∈ p', ∀p' ∈ P', l_e ∈ D)
15         m = Hml(Σ_e l_e), ∀e ∈ p', ∀l_e ∈ D
16         for each link e in p' do
17             search the available wavelength λ with the smallest index in the fiber link e
18             if there is no available wavelength then
19                 block request r
20             else
21                 determine the wavelength, spectrum grid and modulation format
22                 insert optical flow entries to related OF-AGs
23             end
24         end
25     end
26 end
```

Line 2 initializes an empty path set. Line 3 invocates **Algorithm 4** to build the auxiliary graph based on the source/destination nodes of a service request, and stores the path result of the maximum flow in the set P. Lines 4-8 select lightpaths with the residual bandwidth greater than the service request bandwidth from the set P. If there is no available lightpath, we block the service request in lines 9-11. We design the lightpath selection policy named as maximize capacity-over-hops first (MCHF), and contrast it with other two common mechanisms, i.e., maximize capacity first (MCF) and shortest distance first (SDF) (W. Hou et al. (2017a)). Note that, since optical switching nodes have O/E/O conversion capabilities in an opaque WDM optical network, we can use wavelengths on different fiber links along the lightpath. However, O/E/O conversions can increase the end-to-end latency. Hence, we design MCHF algorithm to minimize the traffic congestion with slight O/E/O conversions. We define aforementioned three mechanisms of the path selection as follows:

ACCEPTED MANUSCRIPT

- Shortest distance first (SDF):

$$\mathrm{Min}\left(\sum_{e} l_e, \forall e \in p, \forall p \in P, l_e \in D\right). \tag{27}$$

  We choose the lightpath with the shortest transmission distance from the auxiliary graph derived from **Algorithm 4**.

- Maximize capacity first (MCF):

$$\mathrm{Max}\left(c_f(p), \forall p \in P\right). \tag{28}$$

  We select the lightpath with the largest residual capacity based on Eq. (28). The residual capacity of the path is the minimum residual capacity of all the fiber links along the path, i.e., $c_f(p) = Min\left(c_f(u,v) : e(u,v) \in p\right)$.

- Maximize capacity-over-hops first (MCHF):

$$\mathrm{Max}\left(c_f(p)/hop(p), \forall p \in P\right). \tag{29}$$

  We select the lightpath based on the max-metric which is the value of the residual capacity divided by the hop count of the lightpath. Here, the $hop(\cdot)$ function returns the hop count of the lightpath.

We are able to select the modulation format based on the transmission distance of the lightpath in line 15. Lines 16-24 search the available wavelength λ with the smallest index in the fiber link e, and insert optical flow entries with parameters such as wavelength, modulation level, and spectrum grid to related OF-AGs for establishing the lightpath. If there is no available wavelength, the service request is blocked.

Algorithm 4 constructs the virtual network graph for the service request by continuously increasing the flow value. At the beginning, the initial value given for all links is zero in lines 2-4. During each iteration, increase the flow value of the graph G' by finding an augmented path in the associated residual network graph G'_f. Once we obtain the edge of an augmented path in the graph G'_f, specific edges can be easily identified in G'. Next, modify the flow on these edges to increase the flow value. However, for a particular edge of the graph G', its traffic may increase or decrease. It is necessary to reduce the flow of some edges so that the algorithm can send more flows from the source node to the destination node. In line 6, Breadth-First-Search (BFS) is utilized to calculate the path based on the residual network G'_f. Each residual edge of the path p is either the edge of the original network G' or the opposite edge. Lines 9-17 of the algorithm accordingly update the flow for each case. If the residual edge is the edge of the original network G', increase the flow value, otherwise reduce the flow value. When there is no more augmenting path, the flow is the maximum flow. Finally, we set the flag to zero at the end of the while loop, and return the result of the set P.

4.2. Time Complexity

As the main body, **Algorithm 1** consists of **Algorithm 2 MSECML** and **Algorithm 3 MCHF**. Dijkstra's algorithm has the worst-case time complexity of $O\left(V^2\right)$. We make K calls to

ACCEPTED MANUSCRIPT

Algorithm 4: Find Maximum Flow Paths for s→d

Input: Substrate network G', source/destination nodes s and d.
Output: Lightpaths set P.

1 $P = \emptyset$
2 **for** *each edge* $e(u,v) \in E'$ **do**
3 $\quad f(u,v) = 0$
4 **end**
5 **while** $flag = 1$ **do**
6 $\quad$ calculate the path p from s to d based on $BFS(G'_f, s, d)$ in the residual network G'_f
7 $\quad$ **if** $p \neq \emptyset$ **then**
8 $\quad\quad c_f(p) = Min\left(c_f(u,v) : e(u,v) \in p\right)$
9 $\quad\quad$ **for** *each edge* $e(u,v)$ *in* p **do**
10 $\quad\quad\quad$ **if** $e(u,v) \in E'$ **then**
11 $\quad\quad\quad\quad f(u,v) = f(u,v) + c_f(p)$
12 $\quad\quad\quad\quad P = \{p\}$
13 $\quad\quad\quad$ **end**
14 $\quad\quad\quad$ **if** $e(u,v) \notin E'$ **then**
15 $\quad\quad\quad\quad f(v,u) = f(v,u) - c_f(p)$
16 $\quad\quad\quad$ **end**
17 $\quad\quad$ **end**
18 $\quad$ **end**
19 $\quad$ **if** $p = \emptyset$ **then**
20 $\quad\quad flag = 0$
21 $\quad$ **end**
22 $\quad$ return P
23 **end**

Dijkstra's algorithm in lines 3-6, hence the time complexity becomes KV^2. The worst time complexity occurs in lines 7-25, which is $KV + KN^2 + N$. Hence, the time complexity of **Algorithm 2** is $O\left(KV^2 + KV + KN^2 + N\right)$. We use the BFS algorithm to find the augmented path in line 6 of **Algorithm 4**, which has the time complexity of $O\left(E'^2\right)$. Since the total number of executions of the flow increment operation is $O(V'E')$, the time complexity of **Algorithm 4** is $O\left(V'E'^2\right)$. In addition, lines 16-24 of **Algorithm 3** consume $E'W$ time at the worst case. Thus, the time complexity of **Algorithm 3** is $O\left(V'E'^2 + E'W\right)$. In summary, the total time complexity of the main body is approximate $O\left(KV^2 + KN^2 + V'E'^2 + KV + E'W + N\right)$, which is polynomial.

5. Experimental demonstration and results discussion

We first introduce the simulation setup. Next, we experimentally demonstrate the feasibility of proposed solutions in a semi-practical platform. Finally, the algorithm performance is evaluated quantitatively.

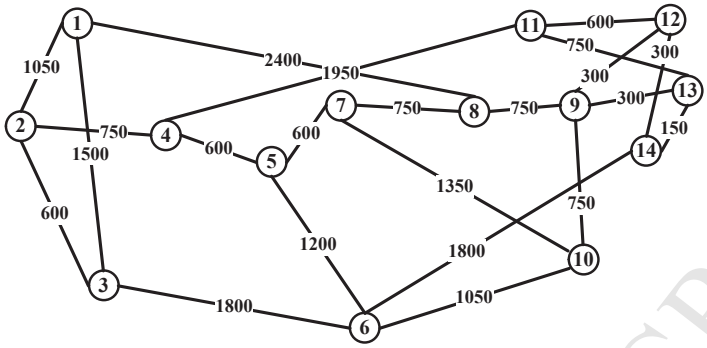

Figure 4: The NSFNET topology used in simulations.

5.1. Simulation Setup

The simulation topology NSFNET is shown in Fig. 4. The number on the link indicates the distance. Both the feasibility of the overall solution and the effectiveness of algorithms are performed in NSFNET including 14 nodes and 22 bidirectional fiber links. The testbed of software-defined multi-granularity optical networks (SD-MGON) is built with RYU controller and Mininet. The Mininet simulates OF-AGs attached to optical switching devices, and the more detailed OF-AG structure can be found in our previous work (X. Zhang et al. (2017a)). Though there is no real expensive BV-OXC or BV-WSS, we assign virtual hardware resources (i.e., 2 processors, 4 GB memory and 1 network adapter) to each node via Mininet running on Ubuntu operating system. The software-defined and multi-granularity routing application is developed on the extended RYU controller.

The network parameters in transparent and opaque domains are set separately. For the transparent domain, the total bandwidth for each link is 4000 GHz, and each link occupies the frequency band of 192.1 THz to 196.1 THz. A single fiber link carries 320 frequency slots each with the size of 12.5 GHz. The bandwidth requirement of flexi-grid service requests includes five types: 10 Gbps, 50 Gbps, 100 Gbps, 400 Gbps, and 1000 Gbps (super wavelength). Service requests are randomly distributed with the equal probability. For the opaque domain, the initial bandwidth provisioning of the wavelength is OC-96, i.e., 96 optical carriers. Each fiber link has 16 wavelengths each with 50 GHz spectrum grid. All service requests have the same bandwidth requirement, i.e., one wavelength. Moreover, our system supports four modulation levels: BPSK, QPSK, 8-QAM and 16-QAM. The maximum reach of the lowest modulation level BPSK is 3000 km, while the one of the highest modulation level 16-QAM is 700 km.

5.2. Experimental Demonstration

First, we show the internal functional components of software-defined multi-granularity routing application in Fig. 5, mainly including the modules of network awareness, resource discovery, request analysis, route computation, spectrum allocation, optical flow delivery and traffic engineering database.

Network awareness and resource discovery modules (i.e., NAM and RDM) collect the information of network topology and element resource, respectively. They discover network nodes and resource information through communicating with the optical agent using extended Open-

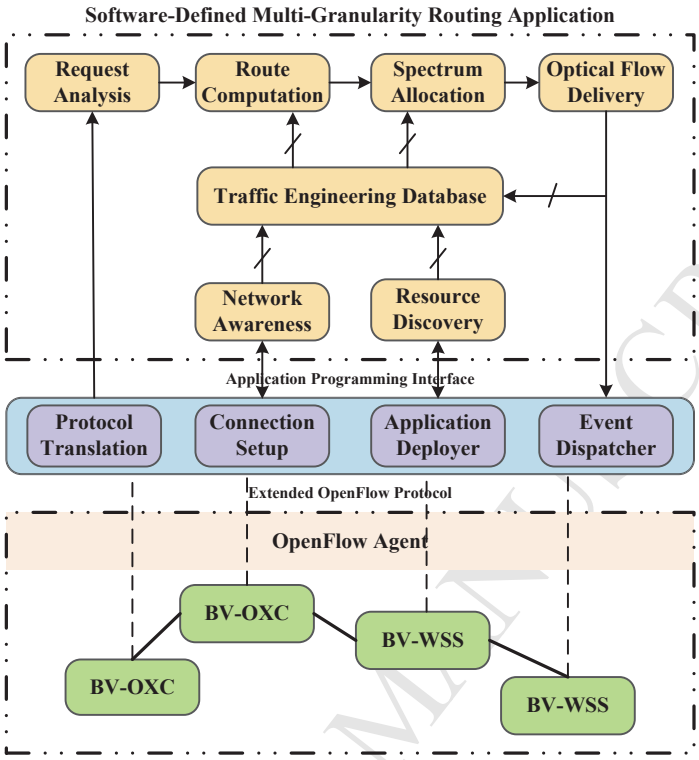

Figure 5: Software-defined multi-granularity routing application.

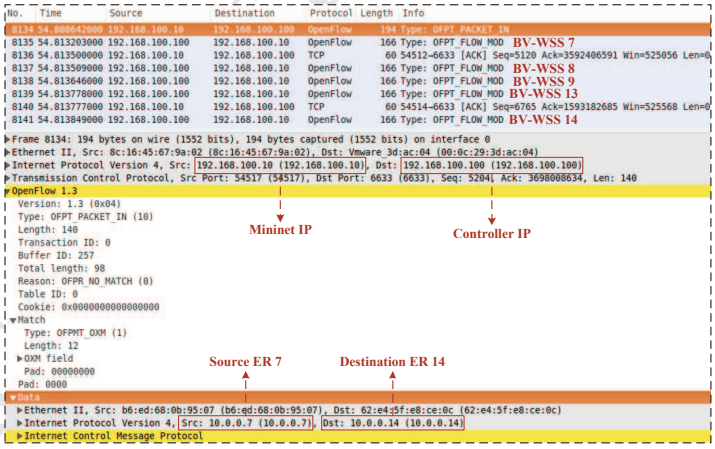

Figure 6: Wireshark capture for establishing a lightpath in the transparent domain.

Flow protocol. They also sense the inter-node link connection information by sending messages to all the nodes interconnected with them.

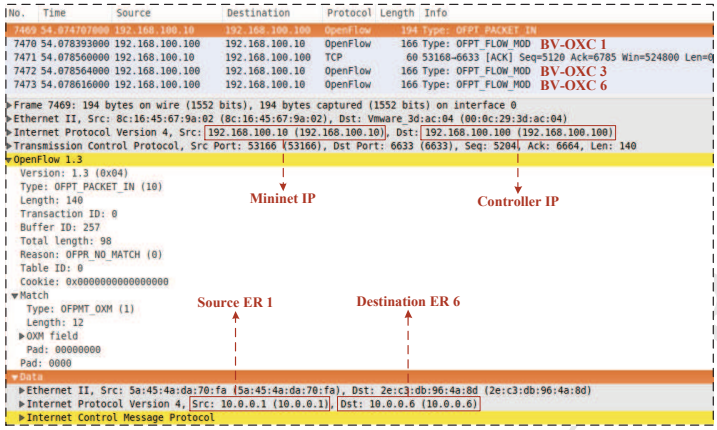

Figure 7: Wireshark capture for establishing a lightpath in the opaque domain.

The service request analysis module (RAM) analyzes the source address, destination address, and communication capacity according to the received service request, and reporting them to the route computation module (RCM). The requests of different granularity types are also distinguished here. The RCM performs the above-mentioned path calculation algorithm to determine eligible candidate lightpaths according to the service request information provided by RAM and the network topology resource information provided by the traffic engineering database module (TED). After that, RCM transmits the routing information to the spectrum allocation module (SAM) where the optimal spectral distribution scheme can be invoked.

The SAM receives the occupancy status of frequency slots provided by TED and the candidate routing information sent by RCM. SAM allocates the modulation format according to the candidate route length, and implements the optimal spectral distribution scheme based on our designed algorithms. In addition, it also sends the result of the spectral distribution scheme to the optical flow table delivery module (FDM). FDM constructs the optical flow table according to the result of routing and resource allocation, and it also has the ability to send optical flow entries to related OF-AGs along the lightpath. Furthermore, it also updates the resource usage information in TED after serving a service request.

The TED module obtains real-time network link state information and stores the abstract mapping results for the underlying network resources, including optical nodes, fiber link relationships, lengths among nodes, and the spectrum occupancy of each link, etc., which facilitates the centralized network management and control. This module also has topology query and information update functions. The topology query function can provide the link status information for both RCM and SAM. After the resource allocation is completed, the existing network topology and resources information are updated so that the network status obtained by the next service request is real-time and reliable.

Next, the procedure of the software-defined and multi-granularity routing application is described as follows:

- **Step 1**: A service request arrives at the ER.
- **Step 2**: The OF-AG on the ER sends an extended Packet-In message to the controller.

ACCEPTED MANUSCRIPT

- **Step 3**: RAM receives the Packet-In message and analyzes the type of the service request.
- **Step 4**: RCM obtains the network status from TED, and invokes the corresponding path calculation algorithm for different types of services. The modulation format of the lightpath is also determined based on the path length.
- **Step 5**: SAM performs the optimal spectrum allocation scheme after receiving candidate paths from RCM. Note that, Algorithms 2 and 3 may be required to provide the network service for multi-granularity requests according to the network status provided by TED.
- **Step 6**: If a feasible solution can be obtained, FDM generates corresponding optical flow entries, and insert them to related OF-AGs along the lightpath by utilizing extended Flow-Mod messages.
- **Step 7**: The OF-AG parses the optical flow entry and configures the underlying BV-OXC or BV-WSS in the data plane to setup the lightpath.
- **Step 8**: If the lightpath is successfully established, FDM updates the resource status information for TED.

Finally, we experimentally demonstrate the feasibility of performing software-defined multi-granularity routing applications on our semi-practical system platform. Based on the NSFNET topology, we make experiments to establish lightpaths with MSECML and MCHF algorithms, which can verify basic system functionalities. Figures 6 and 7 show the wireshark captures for establishing lightpaths in transparent and opaque domains, respectively, in the manner of recording related OpenFlow messages. As shown in Fig. 6, a lightpath containing 5 hops (i.e., BV-WSS 7→BV-WSS 8→BV-WSS 9→BV-WSS 13→BV-WSS 14) is established in the transparent domain. Figure 7 shows that a three-hop lightpath (i.e., BV-OXC 1→BV-OXC 3→BV-OXC 6) is built into the opaque domain. Furthermore, Flow-Mod messages are captured in Figs. 8 and 9. In Fig. 8, we can observe that the central frequency, slot width and modulation format fields are extended to set up the optical flow entry in the transparent domain. The central frequency used by the service request is 192.15 Thz, and 8 spectrum slots are occupied when using the QPSK modulation format. The wavelength, spectrum grid and modulation format are also found for the opaque domain in Fig. 9. The wavelength assigned to the request by the application is 1552.52 nm, and the fixed granularity of the spectrum channel is 50 GHz.

5.3. Performance Evaluation

We evaluate the performance of proposed algorithms in transparent and opaque domains, respectively.

5.3.1. Performance for transparent domain

To evaluate the effect of the proposed algorithm MSECML, the comparison algorithms and abbreviations used in this paper are as follows: (1) Minimize the spectrum slot number (MSSN) (K. Christodoulopoulos et al. (2010)) based on first fit spectrum allocation without considering adaptive modulation format. (2) Minimize the spectrum slot number with modulation level (MSSNML) (Z. Zhu et al. (2013)). The appropriate modulation format is automatically selected according to the path length.

Figure 10 shows the average spectrum efficiency versus the service request. The spectrum efficiency of MSECML is not much different from MSSNML, and it floats up and down at 3.5

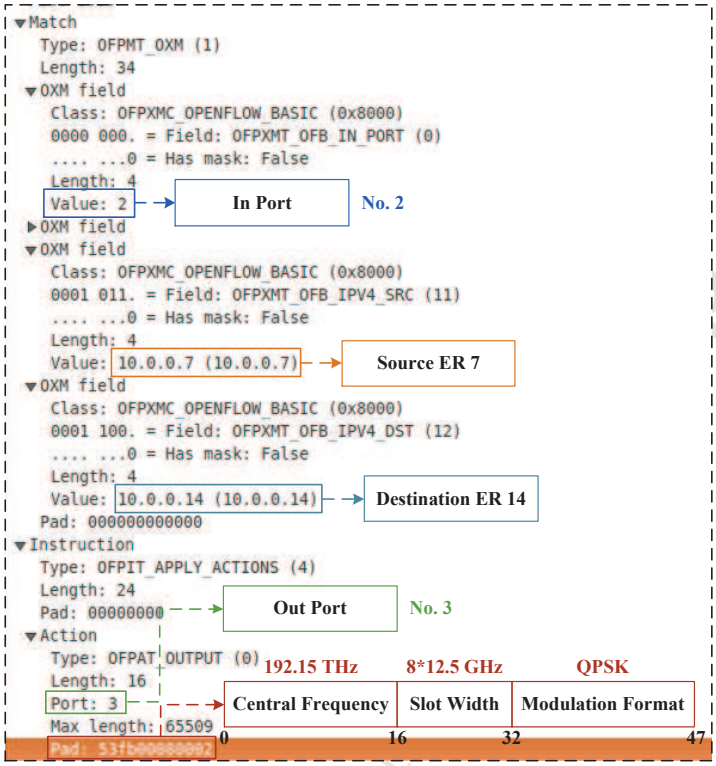

Figure 8: Wireshark capture of a Flow-Mod message in the transparent domain.

bps/Hz, but it is 1.8 times the spectral efficiency of MSSN. This is because that both MSECML and MSSNML can automatically select the modulation format based on the path distance, which increases the channel capacity of each subcarrier. Moreover, when the number of services exceeds 350, the increase of MSECML algorithm is higher than MSSNML, so it is more suitable for large traffic scenarios.

Figure 11 shows the effect of the number of service requests on the network throughput. With the increasing number of service requests, the network throughput follows an upward trend. When the number of requests is in the range of 50 to 150, the throughput of three algorithms is similar because the network can satisfy the small bandwidth requirement of services. When the range is 150-350, the throughput of MSSNML and MSSN is very similar, but MSECML still well accepts services with the corresponding throughput significantly greater than other two algorithms. The reason for this result is that MSSNML and MSSN have some blocked connections as the number of services rises, leading to a slow increase of the network throughput. When the number of services is greater than 350, the throughput growth of MSSN becomes slow, while MSSNML remains basically linear, because the network rejects service requests when using MSSN. As the number of services continues to increase, the network throughput gradually approaches the limit of the network capacity. The MSECML always maintains a high value, so it has an obvious advantage in improving the network throughput.

Figure 12 shows the impact of the number of services on the blocking probability. As the

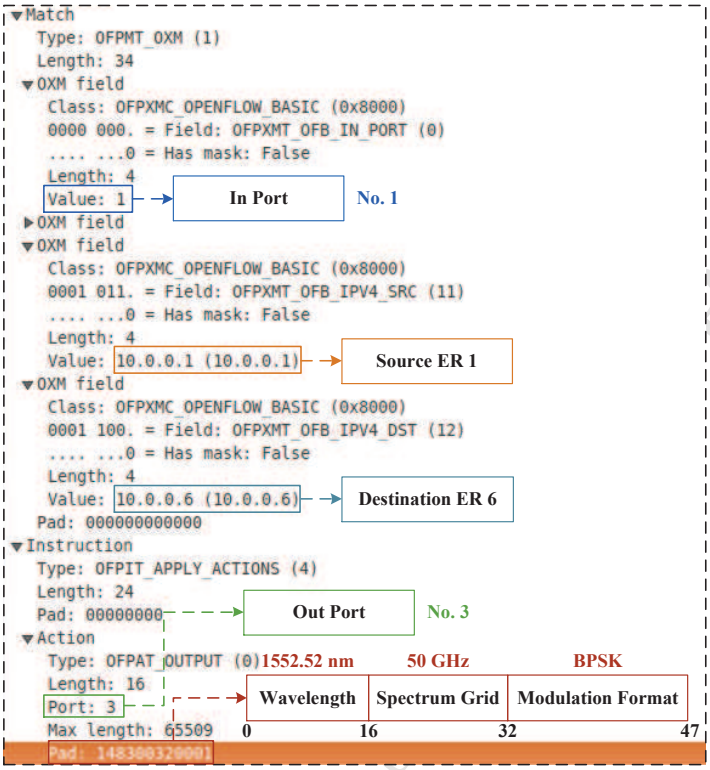

Figure 9: Wireshark capture of a Flow-Mod message in the opaque domain.

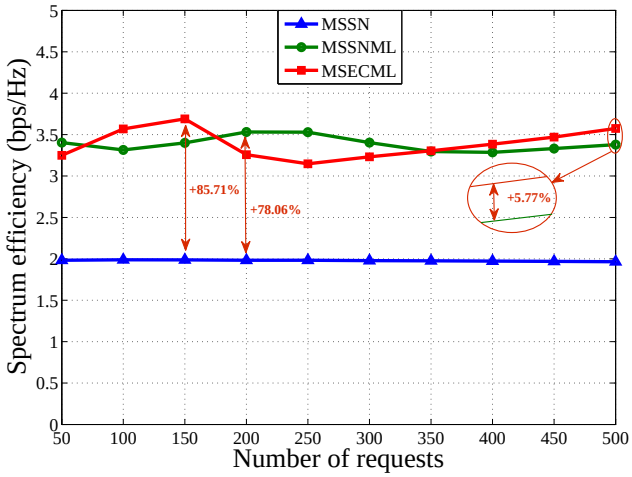

Figure 10: Spectrum efficiency in the transparent domain.

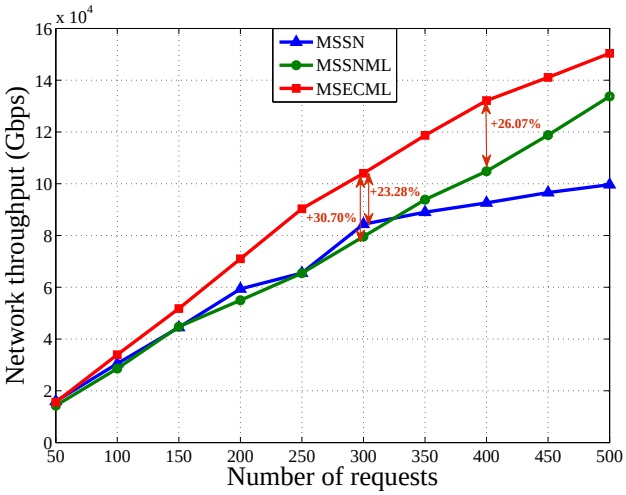

Figure 11: Network throughput in the transparent domain.

increasing number of requests arriving at the network, due to limited resource provisioning, there will be more refused services without establishing connections in a short period of time. When the number of service requests exceeds 300, the blocking probability of MSSN shows a sharp increase, even 10%. In addition, for MSSNML line, there is a drop at the request number 450, and the blocking probability seem to be saturated from 359-500 without any further obvious increasing. The reason for this phenomenon is related to the traffic of 450 randomly generated requests. Due to random and dynamic traffic, there is a slight drop at this point. However, from a statistical point of view, the blocking rate still shows an upward trend because the redundant bandwidth is gradually consumed. In three algorithms, MSECML achieves the lowest blocking probability because it uses a flexible modulation format selection method to better utilize network resources for the lightpath establishment.

Figures 13 and 14 show the blocking probability and network throughput with different k values, respectively. It is obvious that a larger k can achieve the lower blocking probability or the higher network throughput. The network throughput when k=5 is approximately 13.36% higher than that when k=2. The reason for this result is that the more candidate paths and spectrum blocks are available when k=5, which improves the network ability to carry services. However, a large k inevitably leads to a long processing delay, shown in Fig. 15. We can see that the average latency when k=5 is reduced from 35 milliseconds to 25 milliseconds, which is the result of repeatedly using the flow table. The average delay when k=2 is maintained at more than ten milliseconds, which is about 20 milliseconds shorter than the average delay when k=5 because the corresponding RCM performs fewer cycles.

5.3.2. Performance for opaque domain

In the opaque domain, we evaluate the performance of the proposed MCHF algorithm, SDF and MCF (W. Hou et al. (2017a)). Figure 16 shows the blocking probability versus the number of requests. Three curves have the same variation trend but MCHF has the lowest blocking probability. We can also observe that the blocking probability of MCHF is slightly lower than

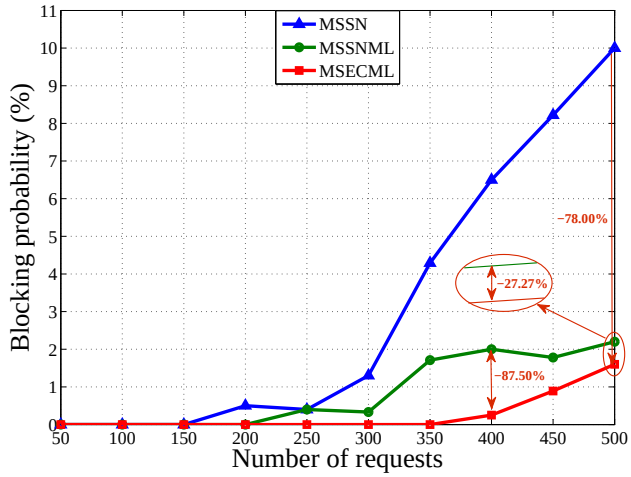

Figure 12: Blocking probability in the transparent domain.

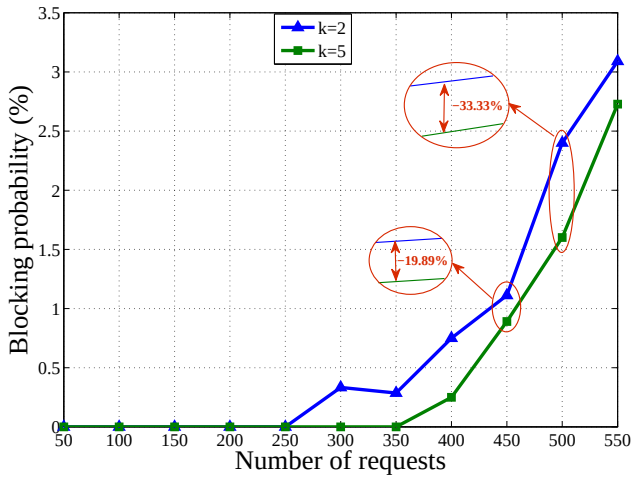

Figure 13: Blocking probability with different k values in the transparent domain.

SDF when the number of requests is in the range of 400-500. This is because that the number of service requests has exceeds the limit of the network capacity. The network throughput is shown in Fig. 17 where MCF has the lowest value. The MCHF throughput is slightly lower than SDF when there are 50-250 requests, which is caused by prioritizing short distance paths using high modulation levels at the scenario of light network load. However, as the traffic continues to increase, the advantage of MCHF gradually becomes obvious, and MCHF throughput is 18.64% higher than MCF when there are 400 requests.

Figure 18 shows the total transmission distance with different numbers of service requests.

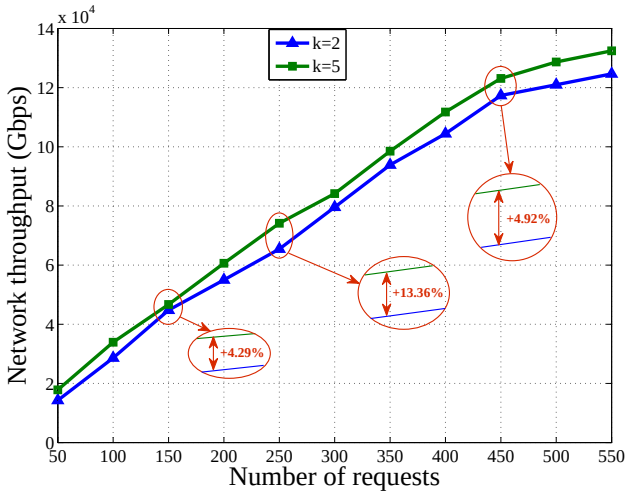

Figure 14: Network throughput with different k values in the transparent domain.

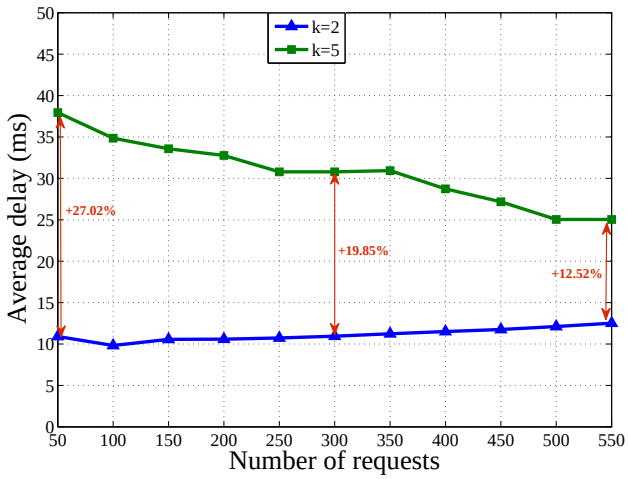

Figure 15: Average delay with different k values in the transparent domain.

The total transmission distance of SDF is the shortest because it always chooses the shortest lightpath, but MCF has the longest distance because MCHF can achieve a desirable distance while ensuring a larger network throughput. Furthermore, the total transmission distance increases approximately linearly when the number of requests is from 50 to 250, and after 250, it tends to be flat due to the gradual saturation of the network capacity.

In Fig. 19, the spectrum efficiency of the wavelength using BPSK modulation format is 2 bps/Hz, and obviously 4, 6 and 8 bps/Hz for QPSK, 8-QAM and 16-QAM, respectively. When the number of services is in the range of 50-300, SDF has the highest spectrum efficiency, but

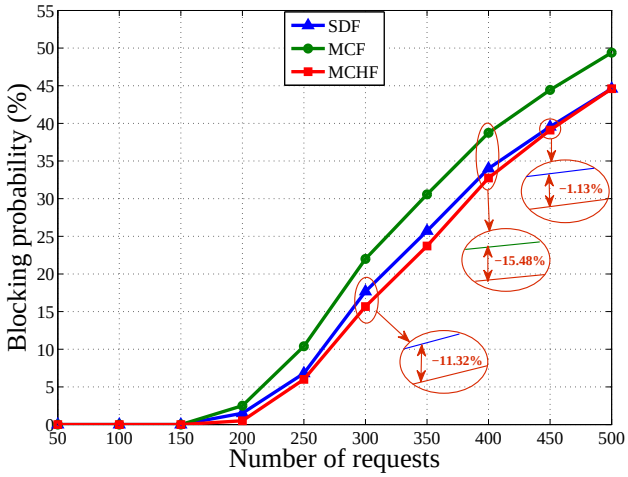

Figure 16: Blocking probability in the opaque domain.

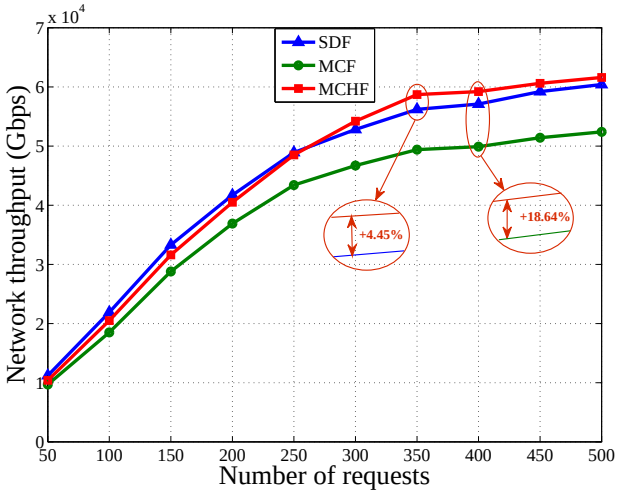

Figure 17: Network throughput in the opaque domain.

from 300 to 500, MCHF performs better than SDF. This phenomenon can be explained as follows. Under the scenario of the light load, the lightpath with short distance can have higher spectrum utilization, but with the increasing number of services, SDF results in severe network congestion, leading to the decrease of the average spectrum efficiency. In contrast, MCHF improves the spectrum efficiency while carrying more services.

Finally, we analyze the end-to-end delay in the opaque domain, from the perspectives of average number of O/E/O conversions and average transmission distance because they are positively related to the transmission delay. Figure 20 shows the average number of O/E/O conversions.

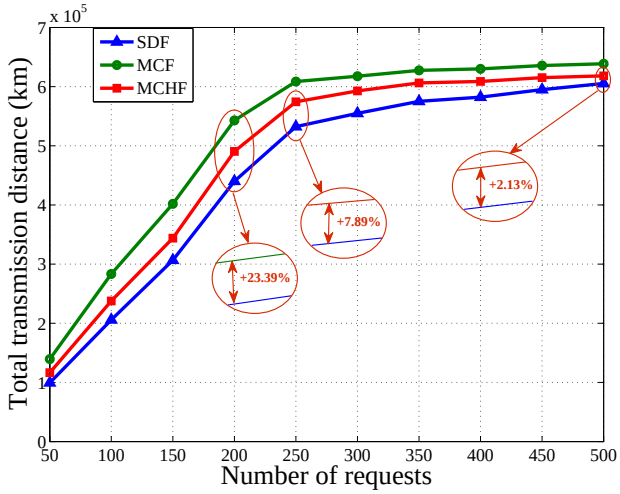

Figure 18: Total transmission distance in the opaque domain.

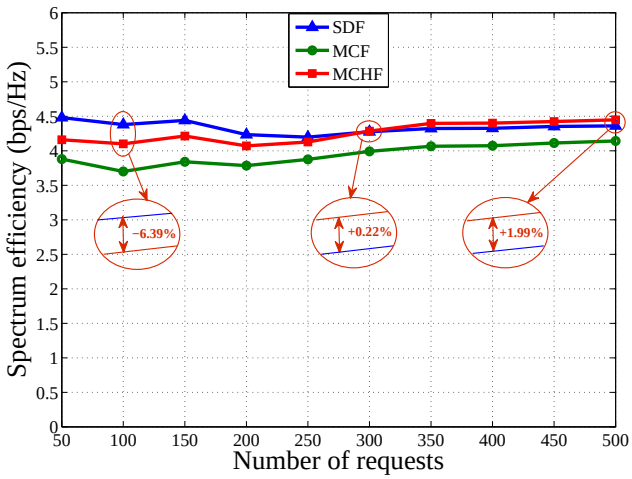

Figure 19: Spectrum efficiency in the opaque domain.

MCHF has the fewest O/E/O conversions, and its peaks and troughs are 1.21 and 0.79 times, respectively. However, MCF has the highest average number of O/E/O conversions, which inevitably increases the transmission latency because the O/E/O conversion takes more time to complete. In addition, the average frequency of O/E/O conversions in MCHF is decreased by 3.13% compared to SDF. Moreover, from Fig. 21, the average transmission distance of MCHF is slightly higher than SDF. It is noteworthy that the speed of light transmission in the optical fiber is very fast, and a small distance difference does not bring a large transmission delay. On the contrary, the O/E/O conversion consumes a large part of the transmission delay. Therefore, the

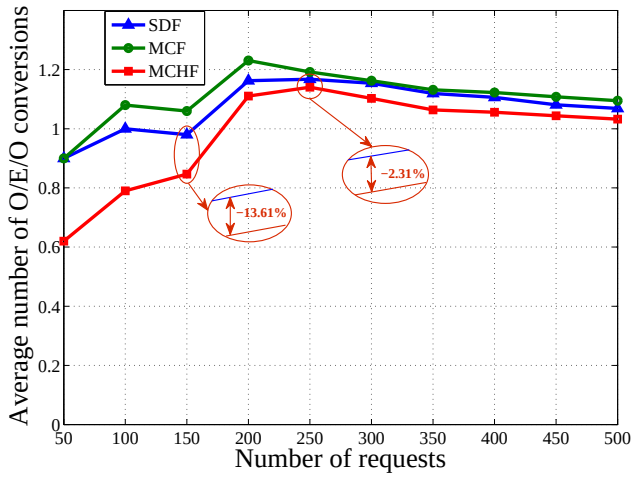

Figure 20: Average number of O/E/O conversions in the opaque domain.

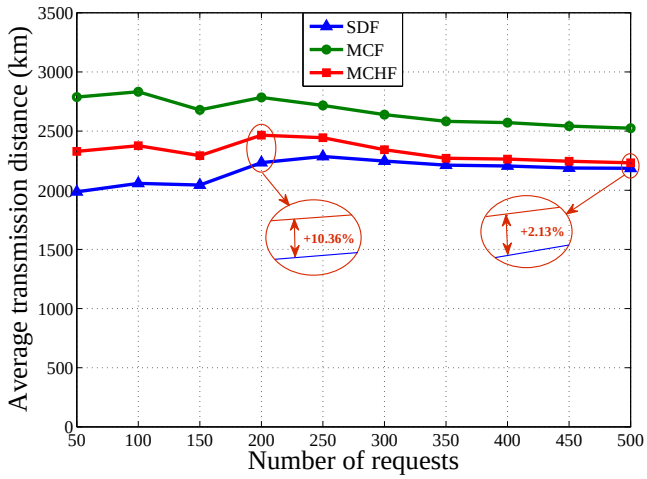

Figure 21: Average transmission distance in the opaque domain.

effect of O/E/O conversions on transmission delay plays a decisive role. In summary, our MCHF has the better performance.

6. Conclusion and future work

Cleaner production will be an important means of implementing sustainable development. For a large number of population problems in the future, building smart and sustainable cities will be able to effectively use urban resources to reduce or eliminate their possible harm to the

ACCEPTED MANUSCRIPT

environment, while fully satisfying human needs and maximizing social and economic benefits. The effective data delivery mechanism proposed in this paper will promote the city to develop in a more intelligent direction. It will also encourage the coordinated and sustainable development of the city's economy, society, and environment, which will accelerate the goal of cleaner production and improve the quality of urbanization.

In this paper, we have investigated the SPTS-SDMGON problem in transparent and opaque domains, respectively, based on the overall software-defined and multi-granularity inter-DC network architecture. Especially, we developed software-defined multi-granularity routing applications on the RYU controller, and implemented seamless operation between control and data planes by extending the OpenFlow protocol. However, using traditional path planning algorithms, it is difficult to give an optimal traffic scheduling solution based on the dynamic status of link load in real time. In the future, based on historical massive traffic data, we will use artificial intelligence technology (AI) to actively predict and effectively schedule the traffic carried on the link. It also has the ability to collect the massive amount of data from the data plane in real time. In the future, through the introduction of AI technology, applications can use the big data collected by controllers for deep learning, which is able to realize active network optimization and predictive operation and maintenance.

Acknowledgements

This work was supported in part by the National Nature Science Foundation of China under Grant 61502075, Grant 61501104, Grant 61775033 and Grant 61771120, and in part by the Fundamental Research Funds for the Central Universities under Grant N161604004, Grant N161608001, Grant N171602002, and Grant DUT17RC(4)49.

References

A. Coiro et al., 2014. Energy-Efficient Routing and Wavelength Assignment in Translucent Optical Networks. IEEE/OSA Journal of Optical Communications and Networking 6, 843–857.

A. N. Patel et al., 2013. QoS-Aware Optical Burst Switching In OpenFlow Based Software-Defined Optical Networks, in: 17th International Conference on Optical Network Design and Modeling, Brest. pp. 275–280.

A. Thyagaturu et al., 2016. Software Defined Optical Networks (SDONs): A Comprehensive Survey. IEEE Communications Surveys & Tutorials 18, 2738–2786.

B. Guo et al., 2011. Dynamic Survivable Mapping in IP Over WDM Network. Journal of Lightwave Technology 29, 1274–1284.

C. Wang et al., 2014. Cellular Architecture and Key Technologies for 5G Wireless Communication Networks. IEEE Communications Magazine 52, 122–130.

D. Kreutz et al., 2015. Software-Defined Networking: A Comprehensive Survey. Proceedings of the IEEE 103, 14–76.

D. Mark et al., 2018. Smart cities: Under-gridding the sustainability of city-districts as energy efficient-low carbon zones. Journal of Cleaner Production 173, 39–48.

F. Musumeci et al., 2013. Dynamic Grooming and Spectrum Allocation in Optical Metro Ring Networks with Flexible Grid, in: 15th International Conference on Transparent Optical Networks, Cartagena. pp. 1–4.

G. Shen et al., 2009. Energy-Minimized Design for IP Over WDM Networks. IEEE/OSA Journal of Optical Communications and Networking 1, 176–186.

H. Shahhosseini et al., 2018. Multi-objective optimisation of steam methane reforming considering stoichiometric ratio indicator for methanol production. Journal of Cleaner Production 180, 655–665.

H. Yang et al., 2015. Performance evaluation of data center service localization based on virtual resource migration in software defined elastic optical network. Optics Express 23, 23059–23071.

J. Vizcano et al., 2012. Energy Efficiency Analysis for Dynamic Routing in Optical Transport Networks, in: IEEE International Conference on Communications, Ottawa. pp. 3009–3014.

ACCEPTED MANUSCRIPT

J. Wang et al., 2013. On the Design of Energy Efficient Optical Networks with Software Defined Networking Control Across Core and Access Networks, in: 17th International Conference on Optical Network Design and Modeling, Brest. pp. 47–52.
J. Zhang et al., 2013. Experimental demonstration of elastic optical networks based on enhanced software defined networking (eSDN) for data center application. Optics Express 21, 26990–27002.
K. Christodoulopoulos et al., 2010. Routing and Spectrum Allocation in OFDM-based Optical Networks with Elastic Bandwidth Allocation, in: IEEE Global Telecommunications Conference, Miami. pp. 1–6.
K. Walkowiak et al., 2017. Influence of Modulation Format Transmission Reach on Performance of Elastic Optical Networks, in: 19th International Conference on Transparent Optical Networks, Girona. pp. 1–4.
L. Cui et al., 2016. When Big Data Meets Software-Defined Networking SDN for Big Data and Big Data for SDN. IEEE Network 30, 58–65.
L. Gong et al., 2014. Virtual Optical Network Embedding (VONE) Over Elastic Optical Networks. Journal of Lightwave Technology 32, 450–460.
L. Guo et al., 2013. Green Provisioning of Many-to-Many Sessions Over WDM Optical Networks. Journal of Lightwave Technology 31, 3289–3301.
L. Guo et al., 2018. Quick Answer for Big Data in Sharing Economy: Innovative Computer Architecture Design Facilitating Optimal Service-Demand Matching. IEEE Transactions on Automation Science and Engineering, DOI: 10.1109/TASE.2018.2838340 .
L. Li et al., 2017. Dynamic State Aware Adaptive Source Coding for Networked Control in Cyberphysical Systems. IEEE Transactions on Vehicular Technology 66, 10000–10010.
L. Liu et al., 2011. Experimental validation and performance evaluation of OpenFlow-based wavelength path control in transparent optical networks. Optics Express 19, 26578–26593.
L. Liu et al., 2013a. Field Trial of an OpenFlow-Based Unified Control Plane for Multilayer Multigranularity Optical Switching Networks. Journal of Lightwave Technology 31, 506–514.
L. Liu et al., 2013b. OpenSlice: an OpenFlow-based control plane for spectrum sliced elastic optical path networks. Optics Express 21, 4194–4204.
L. Ruan et al., 2013. Survivable Multipath Routing and Spectrum Allocation in OFDM-Based Flexible Optical Networks. IEEE/OSA Journal of Optical Communications and Networking 5, 172–182.
M. Channegowda et al., 2013. Experimental demonstration of an OpenFlow based software-defined optical network employing packet, fixed and flexible DWDM grid technologies on an international multidomain testbed. Optics Express 21, 5487–5498.
P. Lu et al., 2017. Data-Oriented Task Scheduling in Fixed- and Flexible-Grid Multilayer Inter-DC Optical Networks: A Comparison Study. Journal of Lightwave Technology 35, 5335–5346.
P. Ramezani et al., 2017. Toward the Evolution of Wireless Powered Communication Networks for the Future Internet of Things. IEEE Network 31, 62–69.
Q. Zhang et al., 2013. RWA for Network Virtualization in Optical WDM Networks, in: Optical Fiber Communication Conference and Exposition and the National Fiber Optic Engineers Conference, Anaheim. pp. 1–3.
W. Hou et al., 2017a. Novel Framework of Risk-Aware Virtual Network Embedding in Optical Data Center Networks. IEEE Systems Journal, DOI: 10.1109/JSYST.2017.2673828 .
W. Hou et al., 2017b. Temporal, Functional and Spatial Big Data Computing Framework for Large-Scale Smart Grid. IEEE Transactions on Emerging Topics in Computing, DOI: 10.1109/TETC.2017.2681113 .
W. Hou et al., 2018a. On-Chip Hardware Accelerator for Automated Diagnosis Through Human-Machine Interactions in Healthcare Delivery. IEEE Transactions on Automation Science and Engineering, DOI: 10.1109/TASE.2018.2832454 .
W. Hou et al., 2018b. Service Degradability Supported by Forecasting System in Optical Data Center Networks. IEEE Systems Journal, DOI: 10.1109/JSYST.2018.2821714 .
W. Lu et al., 2013. Dynamic Service Provisioning of Advance Reservation Requests in Elastic Optical Networks. Journal of Lightwave Technology 31, 1621–1627.
X. Chen et al., 2015. On Spectrum Efficient Failure-Independent Path Protection p-Cycle Design in Elastic Optical Networks. Journal of Lightwave Technology 33, 3719–3729.
X. Wan et al., 2012. Dynamic Traffic Grooming in Flexible Multi-Layer IP/Optical Networks. IEEE Communications Letters 16, 2079–2082.
X. Zhang et al., 2016. Failure Recovery Solutions Using Cognitive Mechanisms for Software Defined Optical Networks, in: 15th International Conference on Optical Communications and Networks, Hangzhou. pp. 1–3.
X. Zhang et al., 2017a. Experimental demonstration of an intelligent control plane with proactive spectrum defragmentation in SD-EONs. Optics Express 25, 24837–24852.
X. Zhang et al., 2017b. Failure Recovery Solutions Using Cognitive Mechanisms Based on Software Defined Optical Network Platform. Optical Engineering 56, 1–14.
Y. Fan et al., 2018. Process efficiency optimisation and integration for cleaner production. Journal of Cleaner Production

ACCEPTED MANUSCRIPT

174, 177–183.
Y. Wang et al., 2013. Path connectivity based spectral defragmentation in flexible bandwidth networks. Optics Express 21, 1353–1363.
Y. Yin et al., 2017. Software Defned Elastic Optical Networks for Cloud Computing. IEEE Network 31, 4–10.
Z. Zhu et al., 2013. Dynamic Service Provisioning in Elastic Optical Networks With Hybrid Single-/Multi-Path Routing. Journal of Lightwave Technology 31, 15–22.
Z. Zhu et al., 2015. Demonstration of Cooperative Resource Allocation in an OpenFlow-Controlled Multidomain and Multinational SD-EON Testbed. Journal of Lightwave Technology 33, 1508–1514.
Z. Zhu et al., 2018. Build to tenants' requirements: On-demand application-driven vSD-EON slicing. IEEE/OSA Journal of Optical Communications and Networking 10, A206–A215.

ACCEPTED MANUSCRIPT

ACCEPTED MANUSCRIPT

Table 1: List of notations

Notation	Definition
V	The set of BV-WSSs in the transparent flexi-grid domain of the substrate network.
E	The set of bidirectional fiber links used to connect BV-WSSs in the transparent flexi-grid domain.
V'	The set of BV-OXCs in the opaque fixed-grid domain of the substrate network.
E'	The set of bidirectional fiber links used to connect BV-OXCs in the opaque fixed-grid domain.
$e(u, v)$	The link $e \in E$ or E' from u to v, where $\forall u, v \in V$ or V'.
B	The total spectrum bandwidth of each fiber link in the transparent flexi-grid optical network.
B_{FS}	The bandwidth of a frequency slot in the transparent flexi-grid optical network.
B'	The total bandwidth provisioning of all wavelengths deployed in a fiber link.
B'_{λ}	The bandwidth of a wavelength in the opaque fixed-grid optical network.
N	Total number of frequency slots on each fiber link in the transparent flexi-grid domain.
g	The guard bandwidth between different services in the transparent flexi-grid domain.
C_{BPSK}	The capacity of a frequency slot when using BPSK modulation format.
D	The set of all possible lengths of fiber links in the transparent or opaque domain.
l_e	The length of the fiber link e in the transparent or opaque domain.
W	The total number of wavelengths deployed in a fiber link.
m	The index of the modulation level.
λ	The wavelength index $\lambda, \forall \lambda \in [1, W]$ on a fiber link in the fixed-grid domain.
$w_{e,i}$	The starting frequency slot index of the i^{th} spectrum block on the fiber link e.
$z_{e,i}$	The ending frequency slot index of the i^{th} spectrum block on the fiber link e.
R	The set of all service requirements.
r	A service requirement.
s	The source node of a service requirement.
d	The destination node of a service requirement.
x	The type index of the service request.
b_x	The capacity requirement of x-type service requests.
p	The lightpath from s to d.
P	The set of lightpaths from s to d, and $\forall p \in P$.
P_e	The set of lightpaths that use the fiber link e, and $P_e \in P$.

ACCEPTED MANUSCRIPT

Table 2: List of variables

Variable	Definition
α_p^r	A binary variable. It is equal to 1 if the service requirement r is mapped onto the substrate lightpath p, otherwise it is 0.
β_e^r	A binary variable. It is equal to 1 if the service requirement r subscribes the substrate fiber link e, otherwise it is 0.
$\varphi_{e,i}^r$	A binary variable. It is equal to 1 if the service requirement r uses the i^{th} frequency block on the link e, otherwise it is 0.
π^{r_1,r_2}	A binary variable. It is equal to 1 if two requests r_1 and r_2 select the common fiber link, otherwise it is 0.
σ^{r_1,r_2}	A binary variable. It is equal to 1 if the starting frequency slot index of the spectrum block occupied by the service request r_1 is smaller than that of r_2, otherwise it is 0.
$bm_{e,j}$	A binary variable. It is equal to 1 if the j^{th} frequency slot on the fiber link e is used, otherwise it is 0.
$\xi_{e,\lambda}^r$	A binary variable. It is equal to 1 if the service requirement r consumes the wavelength λ on the substrate fiber link e, otherwise it is 0.
ψ_e^r	A binary variable. It is equal to 1 if the service requirement r subscribes the substrate fiber link e in the opaque fixed-grid domain, otherwise it is 0.
w^r	An integer variable that is the index of the starting frequency slot allocated to the request r.
z^r	An integer variable that is the index of the ending frequency slot allocated to the request r.

ACCEPTED MANUSCRIPT